Green Chemistry

PAPER

View Article Online
View Journal | View Issue

Cite this: *Green Chem.*, 2016, **18**, 243

Pee-dots: biocompatible fluorescent carbon dots derived from the upcycling of urine†

Jeremy B. Essner,[a] Charles H. Laber,[a] Sudhir Ravula,[a] Luis Polo-Parada[b] and Gary A. Baker*[a]

Received 28th August 2015,
Accepted 21st September 2015

DOI: 10.1039/c5gc02032h

www.rsc.org/greenchem

We have demonstrated an easy, economic, one-step synthetic route to water-soluble fluorescent carbon dots derived from the thermal upcycling of urine. These "pee-dots" (PDs), which primarily comprise hydrophile-decorated amorphous carbon, exhibit bright, stable, excitation wavelength dependent fluorescence in aqueous solution and are shown to be useful nanoscale labels in cell imaging applications. Cytotoxicity studies demonstrate that these PDs are benign toward model cell lines, even at concentrations as high as 500 μg mL^{-1}. Notably, this approach converts an otherwise useless, negatively-valued byproduct of human life into a value-added nanoscale product while simultaneously pasteurizing the waste stream. The reported PDs proved to be effective nanoprobes for the fluorescence-based detection of heavy metal ions of environmental concern, particularly Cu^{2+} and Hg^{2+} ions which were found to be strong quenchers of their fluorescence. Interestingly, the optical properties and nanoscale dimensions of the PDs are a direct reflection of the diet (*e.g.*, vitamin C or asparagus (sulfur) fortified) followed by the urine donor.

Introduction

The carbon nanodot (C-dot) is a recently established form of nanocarbon which displays unique and valuable optical properties (*e.g.*, excitation wavelength dependent fluorescence, excellent photostability) compared with its carbonaceous cousins, the fullerenes, graphenes, carbon nanotubes, and nanodiamonds.[1–6] Variously (and often arbitrarily) referred to as carbon quantum dots (CQDs) or graphene quantum dots (GQDs), sometimes depending on their level of crystallinity, C-dots offer an attractive eco-friendliness (*e.g.*, biocompatibility, inertness, low cytotoxicity) not shared with other conventional quantum dots, particularly semiconductor-based quantum dots such as those based on CdX (X = S, Se, Te). These properties, plus their ability to act as electron donors or acceptors coupled with their ease of (bio)conjugation, account for their growing interest as candidates in a number of applications ranging from sensing and bioimaging[1–4] to incorporation within photovoltaic devices.[4–6] From the time of their serendipitous discovery a decade ago during the purification of crude carbon nanotubes, researchers have increasingly explored various synthetic pathways for generating C-dots from myriad carbon sources using a wide variety of means. Synthetic approaches for making C-dots can broadly be lumped into two camps: top-down and bottom-up approaches. Top-down approaches, examples of which consist of arc discharge,[7] laser ablation,[8,9] and electrochemical oxidation,[10–14] involve the cleavage of "large" (macroscale) relatively-pure carbon fragments into smaller and smaller particles, eventually resulting in GQDs if the carbon source is highly graphitic in nature to begin with. Bottom-up approaches, on the other hand, essentially involve assembling the C-dots in an atom-by-atom or molecule-by-molecule fashion from carbon-containing molecular precursors, an approach that overwhelmingly yields C-dots that are highly amorphous in nature. Examples of bottom-up methods include combustion or thermal treatment,[15] and templated,[16] microwave-assisted,[17] or hydrothermal growth.[18] Unfortunately, many of these synthetic procedures (both top-down and bottom-up) involve high temperatures, acidic/alkaline conditions, organic solvents, and/or extensive pre- and post-treatment steps which do not embrace the principles of green chemistry. With environmental sustainability becoming an increasing concern, a shift toward developing greener pathways to C-dots is occurring, both in terms of the use of more benign carbon sources as well as employing synthetic methods such as low-temperature thermal treatment and hydrothermal reactions which do not necessitate subsequent functionalization steps. For instance, it has recently been shown that C-dots can be generated through the carbon-

[a]*Department of Chemistry, University of Missouri-Columbia, Columbia, MO 65211, USA. E-mail: bakergar@missouri.edu; Tel: +1 573-882-1811*
[b]*Department of Medical Pharmacology and Physiology, University of Missouri-Columbia, Columbia, MO 65211, USA*
†Electronic supplementary information (ESI) available: Additional figures and experimental details. See DOI: 10.1039/c5gc02032h

ization of various food wastes, including spent coffee grounds and certain fruit peels (*e.g.*, watermelon, pomelo).[19–21] The recouping of spent foods *via* carbonization to C-dots could have the added benefit of reclaiming a waste stream that might otherwise simply find its way into already-overflowing landfills.

Another area of great environmental concern, and one which relates to the conversion of waste material(s) into more valuable products (*i.e.*, "upcycling"), is waste remediation, especially of human sewage. The lack of clean, potable water is one of the most significant worldwide health issues, affecting billions of people who do not have access to safe drinkable water, including devastating numbers who die tragically each year after consuming contaminated water.[22] Even in densely populated and industrialized areas, contaminates are increasingly entering waste streams due to human activity.[22] In general, conventional wastewater treatments and the further development of these treatment facilities to generate a cleaner end-product are intensive and expensive enterprises.[22] Identifying cheaper means for converting human waste streams into more environmentally-friendly forms and their upcycle to value-added by-products are of particular importance. For example, it has already been shown that biochar and activated carbon can be produced from cattle manure.[23,24] More recently, Wei *et al.* showed that C-dots could be synthesized *via* the hydrothermal treatment of shredded office paper.[25] Given these examples, it is entirely plausible that, under the appropriate conditions, raw sewage waste, which primarily comprises cellulose, fecal matter, and urine, can be converted into useful carbon-based materials, adding value and rendering the sewage harmless whilst eliminating certain time-consuming steps in the purification process.

To this end, it should be pointed out that the solid portion of sewage waste can be usefully employed as a source of fuel or fertilizer (indeed, cow/poultry manure has been used as fertilizer for centuries),[26] however, the remaining liquid portion ("yellow water" containing urine) currently finds essentially no useful applications. In fact, despite comprising just 1% of the volume of domestic wastewater, urine contributes a majority of the chemical nutrients: 80% of the nitrogen and nearly half of the phosphates. These nutrients must be removed through multiple energy-intensive steps before the water is clean enough to release back into our rivers and oceans, if they are not to wreck the ecosystem downstream (*e.g.*, algal blooms). Worse, conventional Western plumbing involves the staggeringly wasteful dilution of urine with vast quantities of drinking water (which then combines with "grey water" from household sinks, baths, and wash machines) plus rainwater to make the removal process unnecessarily inefficient and costly. In order to close the nutrient cycle, some have proposed "pee cycling",[27,28] which entails the diversion and pasteurization of human urine for fertilizer, as a possible option for sustainable living. Although this is something of a minority pursuit so far, a number of countries (among them, Sweden, Finland, Denmark, and the Netherlands) are seriously experimenting with this concept, highlighting an evolving mindset regarding how we should utilize energy and resources in our daily lives.

Urine contains a significant amount of urea (~9 g L^{-1}) as a nitrogenous breakdown product of protein metabolism, in addition to lesser quantities of salts (Cl^-, Na^+, K^+) and heterocyclic species (*e.g.*, creatinine, uric acid), suggesting potential as an otherwise discarded carbon source for making nitrogen-doped C-dots. Indeed, Qu *et al.* reported on C-dots displaying a fairly high quantum yield (14% under 420 nm excitation) produced by microwave irradiation of an aqueous solution of urea and citric acid.[17] Finding a productive use for raw urine is attractive not only for deriving economic benefit but also for relieving the current burden placed upon current wastewater treatment, a problem emerging in developed countries today.

The concept of upcycling of waste to prepare industrially significant carbon-based materials has gained significant traction recently. A key early example is the inspiring work of Pol in which conductive carbon microspheres were prepared from waste plastics, including high density polyethylene grocery bags and polystyrene disposable drinking cups, using a solvent-free autogenic process.[29] The Tour group showed that cheap and even negatively-valued sources ranging from Girl Scout cookies to a cockroach leg could be transformed into pristine graphene using a chemical vapor deposition route.[30] Similarly, Müller *et al.* showed that well-ordered graphene monolayers could be grown *via* liquid precursor deposition using human fingerprint residues with identical quality as those derived from ultrapure precursors.[31] Other prominent examples of value-added carbons include hierarchical micro-/mesoporous carbons produced by pyrolysis of used cigarette filters[32] and C-dots made from the hydrothermal treatment of grass[33] and the pyrolysis of hair.[34] Most recently, researchers successfully carbonized dehydrated human urine in a tube furnace under nitrogen at 700–1100 °C to prepare heteroatom (*e.g.*, N, S, Si, P) doped porous carbons that were electrocatalytic for the oxygen reduction reaction (ORR).[35] The current work adds significantly to the scope of these noteworthy efforts by describing a simple approach for upcycling urine into useful fluorescent carbon dots which display negligible cytotoxicity and show excellent potential for both cellular imaging and fluorescence-based sensing applications.

Results and discussion

In this work, we report on the thermal treatment of human urine to upcycle the negatively-valued waste into useful fluorescent carbon dots, which we will refer to as "pee-dots" (PDs). In addition to carbonizing raw urine derived from an unmodified diet, the test subject volunteered to alternatively consume well-defined quantities of either vitamin C supplements or asparagus, on separate occasions over the course of several days, in an attempt to alter the properties of the urine by doping with excess ascorbic acid or sulfur-containing compounds, respectively. The motivation for this "dietary doping" experiment was to attempt to alter the optical features of the resulting carbon dots by either incorporation of an additional known carbon source in the urine or, in the case of an aspara-

gus-rich diet, S-doping of the final nanocarbon. Indeed, the pungent, disagreeable smell associated with asparagus-urine derives from metabolic breakdown products of asparagusic acid. Although the precise details by which asparagusic acid is metabolized are not completely understood, it is known that asparagusic acid is digested to various sulfur compounds like methanethiol, dimethyl sulfide, and dimethyl sulfoxide (Fig. S1 of the ESI† summarizes the primary suspected breakdown products of asparagusic acid).[36–39] Throughout the remainder of this work, we will refer to C-dots derived from an unmodified diet as UPDs ("unmodified pee-dots"), those derived from a diet heavily supplemented with vitamin C as CPDs, and those upcycled from asparagus-urine as APDs.

Detailed synthetic procedures can be found in the Experimental section. Briefly, collected urine was dehydrated at atmospheric pressure on a hotplate, followed by a carbonization step at 200 °C for 12 h to yield a black char-like material which readily redispersed in water. In addition to these experiments, undoped urine samples were also treated for an extended period of 24 h with representative results summarized in Fig. S2† (panels A, D, and E). Following PD clean-up, which comprises centrifugation, filtration, and dialysis steps, orange to dark brown solutions were obtained depending upon the precise nature of the initial urine, as shown in the inset of Fig. 1.

Reports on C-dots generally show featureless UV-vis absorbance spectra in which the absorbance sharply rises as the wavelength decreases toward the UV region,[1,9,15] an observation generally attributed to π–π^* transitions of aromatic sp^2 domains.[17,18,40–42] The PDs display similar spectral profiles to these typically reported, although all three samples display two shoulders (Fig. 1). The UPDs exhibit a shoulder near 330 nm with a minor shoulder at 390 nm. The CPDs show similar features at 330 and 385 nm, as do the APDs at approximately 325 and 400 nm. The citric acid-urea derived C-dots described by Qu and co-workers, which were reported to possess largely graphitic character, displayed two broad absorption peaks at 340 and 405 nm characteristic of an aromatic pi system.[17] The shoulders present in the absorbance spectra of the PDs appear at similar wavelengths as the characteristic peaks for the citric acid-urea derived C-dots, pointing to a minor graphitic character for the PDs.

All three PD samples displayed fluorescent properties akin to known C-dots, such as excitation wavelength dependent emission, with the APDs showing the most red shifted emission for a given excitation wavelength. As shown in Fig. 2A,

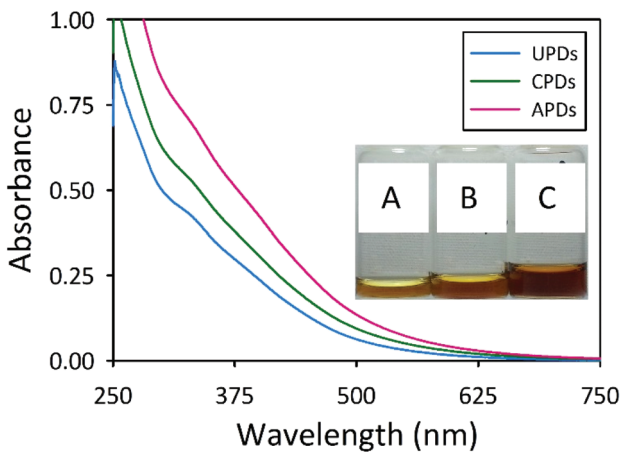

Fig. 1 UV-Vis spectra of the PDs dispersed in water at a concentration of 0.1 mg mL^{-1}: UPDs (cyan curve), CPDs (green curve), and APDs (magenta curve). The inset images show representative samples of (A) UPDs, (B) CPDs, and (C) APDs at the same concentration viewed under ambient light.

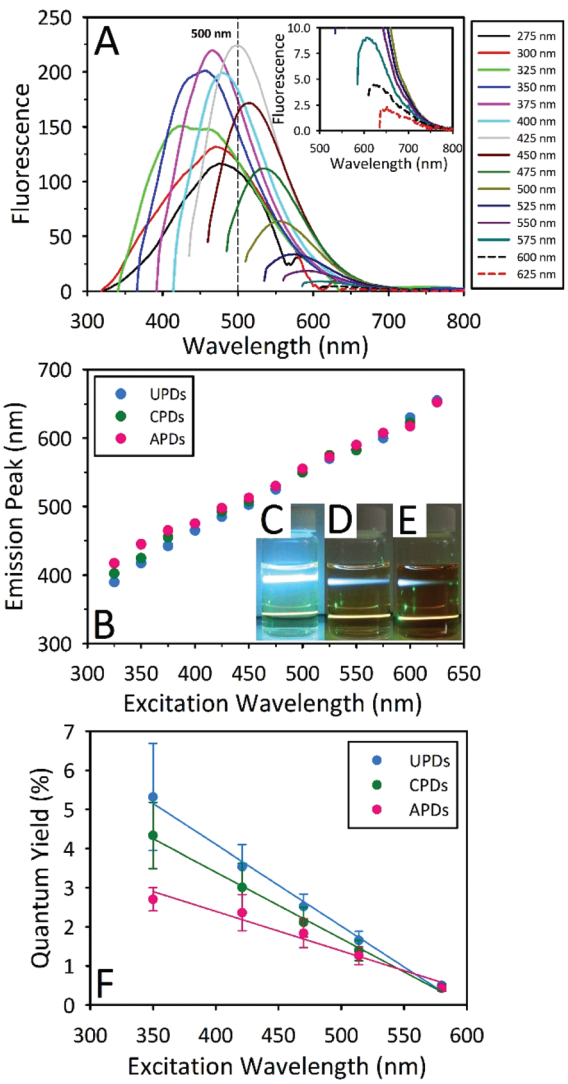

Fig. 2 (A) Excitation wavelength dependent fluorescence emission spectra of APDs in water. Magnified emission spectra at longer excitation wavelengths are displayed in the inset. (B) By plotting the wavelength of maximum emission against the excitation wavelength for these PDs, a red shifted emission for CPDs and APDs relative to UPDs can be seen for shorter excitation wavelengths, particularly below 450 nm. The inset images show the fluorescence of (C) UPDs, (D) CPDs, and (E) APDs under blue (405 nm, upper beam) and green (532 nm, lower beam) laser pointer excitation. (F) Wavelength dependent quantum yields measured at five different excitation wavelengths.

APDs show their peak emission intensity at 500 nm which coincides with 425 nm excitation. In comparison, CPDs (Fig. S2C†) and UPDs (Fig. S2B†) display their highest emission intensities at 427 nm and 392 nm, which correspond to 350 nm and 325 nm excitation, respectively. This easily observable red shift in the emission for the APDs can be traced to the dietary presence and putative incorporation of sulfur into the PDs. A comparison between the wavelength-dependent fluorescence features of the PDs can be made on the basis of a plot illustrating the dependence of the maximum emission wavelength on the excitation wavelength, as shown in Fig. 2B. These data reveal that, to a lesser extent, the CPDs also show a slight red shift relative to UPDs and, moreover, that the red shift is predominant at lower excitation wavelengths, particularly in the UV. Indeed, when the excitation wavelength exceeds 450 nm, the emission-excitation profiles for all three PDs begin to converge.

In order to make direct comparisons with fluorescence quantum yields (QYs) previously reported in the open literature, QYs for these samples were determined for 350 nm excitation using quinine sulfate as the reference fluorophore. Although this is the most popular choice for the determination of C-dot QYs by a wide margin, it is not a particularly meaningful one given the limitations of 350 nm (*i.e.*, UV) excitation in prospective bioimaging applications. That is to say, a high QY value measured for 350 nm excitation does not necessarily translate to a high QY for excitation at longer wavelengths better suited to cellular imaging, a feature underlined by the characteristic drop in the fluorescence intensity from C-dots as the excitation wavelength increases. In order to better elucidate this behavior, we performed a multi-excitation wavelength QY study for the three kinds of PDs using excitation wavelengths of 350, 421, 470, 514, and 580 nm. To the best of our knowledge, this is the first time such a study has been carried out for a multiplicity of excitation wavelengths for C-dots. In fact, only rarely have QYs for C-dots been measured at more than a single excitation wavelength.[17] Our results presented in Fig. 2F demonstrate a clear trend of diminishing QY values as the excitation wavelength increases. Overall, UPDs display the highest QYs (5.3% at 350 nm), with CPDs and APDs presenting lower values, although their maximal QYs similarly occur at 350 nm excitation, with QYs of 4.3% and 2.7%, respectively. Despite this situation, at an excitation wavelength of 580 nm, all three samples display similar QY values (UPDs: 0.50 ± 0.05%, CPDs: 0.44 ± 0.09%, APDs: 0.43 ± 0.07%), an outcome likely related to the red shifted emission associated with the APDs. It should also be noted that the fluorescence emission of UPDs prepared by thermal treatment for 24 h displays a greater red shift compared with samples treated for 12 h. For a 24 h thermal step, the peak emission was observed at 445 under 350 nm excitation while the corresponding UPDs prepared by a 12 h thermal process peaks at 392 nm under 325 nm excitation (Fig. S2,† panel A).

In order to define the nature of the carbon comprising the different PDs, X-ray diffraction (XRD) patterns and Raman spectra were collected for the freeze-dried materials. The

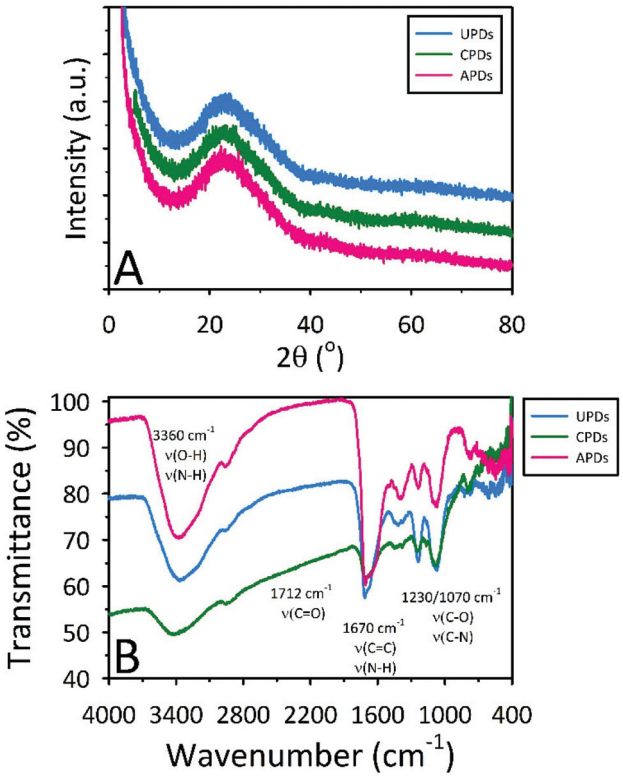

Fig. 3 (A) XRD patterns and (B) FTIR spectra showing the slight graphitic nature and surface functionalities of the PDs, respectively.

powder XRD patterns for all three samples reveal a broad band at approximately 22° with a *d*-spacing between the (002) planes of 0.37–0.38 nm, indicating that the PDs consist of weakly graphitic crystallinity (Fig. 3A). This *d*-spacing also indicates the presence of functional groups on the surface of the slightly graphitic sheets within the dot. This kind of behaviour has been observed in the literature and shows that the PDs are highly amorphous in nature but do possess a slight graphitic nature.[43] The Raman spectra (data not shown) gave no evidence for their graphitic nature, consistent with earlier reports on other C-dots.[44] Although no Raman peaks were discernible for the PDs, the steady increase in intensity with increasing Raman shift has been observed in other C-dots and most certainly arises from their luminescence which could obscure weak graphitic signals.[45]

FTIR spectra for the three different PDs (Fig. 3B) indicate that the PDs are functionalized with carboxyl, carbonyl, hydroxyl, epoxy, and amine moieties. The large, broad absorption band near 3400 cm^{-1} is assigned to the stretching vibrations of O–H (ν_{O-H}) and N–H (ν_{N-H}). The well-defined absorbance bands at 1712 cm^{-1} and 1670 cm^{-1} are ascribed to the stretching vibrations of C=O ($\nu_{C=O}$) and the skeletal vibrations of aromatic groups ($\nu_{C=C}$) or NH/NH_2 deformation (ν_{N-H}), respectively. The peaks at 1230 and 1070 cm^{-1} arise from the different stretching modes of carboxylic, ester, ether, and alcohol moieties (ν_{C-O-C} and ν_{C-OH}), while the peaks near 2950 and 1400 cm^{-1} are assigned to aliphatic carbon

vibrations (ν_{C-H}). These chemical functionalities account for the excellent water dispersibility of PDs while also providing evidence for some degree of conjugation, consistent with the slightly graphitic character suggested by the XRD results.

Representative TEM images for the UPDs, CPDs, and APDs, along with their size histograms are provided in Fig. 4. From Fig. 4A, it can be seen that the thermal treatment of unmodified urine results in UPDs varying in size between 10 and 30 nm, with a few errant particles as large as about 55 nm. The inset provided in Fig. 4A reveals a single large quasi-spherical dot approximately 55 nm in diameter; due to the fact that no discernible lattice fringes can be observed, this image further supports the earlier notion that these PDs are primarily amorphous in nature. The average size of the CPDs is roughly half that of the UPDs (Fig. 4B). Interestingly, the APDs display a bimodal size distribution, with one distribution centered near 17 nm and a second particle size near 55 nm (Fig. 4C). An unanticipated finding, it appears that dietary doping can influence not only the optical properties of the PDs but their size distribution as well.

The three different PDs were next explored for bioimaging studies using mice embryonic fibroblast (MEF) cells (Fig. 5) and BT-474 human mammary gland breast/duct carcinoma cells (Fig. S3†). Despite their modest QY values for visible excitation (in the range of a few percent), the PDs proved fully capable of fluorescently staining both cell lines, demonstrating

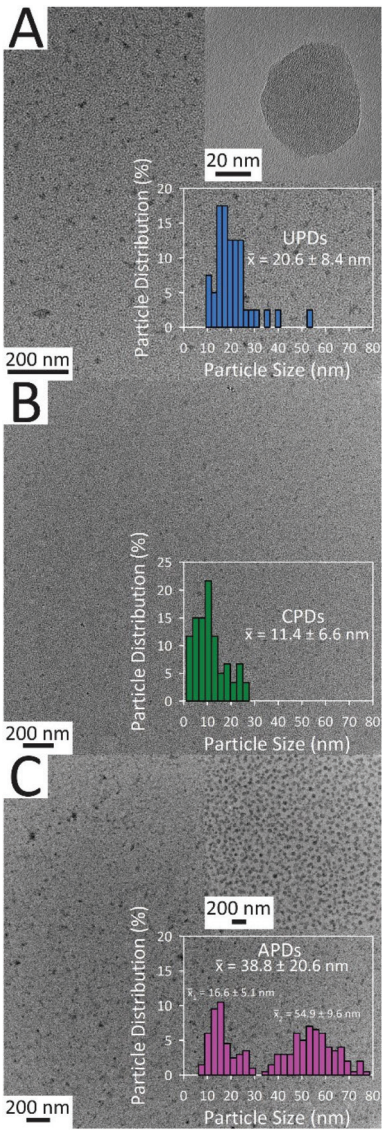

Fig. 4 Respective TEM images of (A) UPDs, (B) CPDs, and (C) APDs. Histograms with the average particle sizes (x-bar) are also shown. The inset of image (C) further illustrates the bi-modal particle size distribution of the APDs.

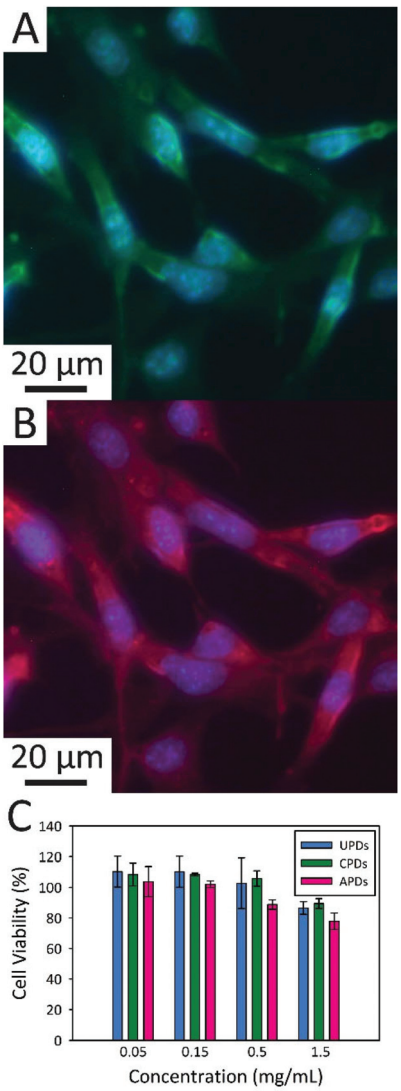

Fig. 5 Merged fluorescence micrographs of APD-incubated mice embryonic fibroblast (MEF) cells showing APD incorporation into the cellular cytoplasm. The cell images combine the signal from DAPI staining of the nuclear material with APD-derived signal collected through a (A) FITC or (B) TRITC filter cube. (C) Summary of BT-474 cell viability for varying concentrations of the three kinds of PDs using a sulforhodamine B cell protein dye-binding assay.

their potential in cell imaging. The fluorescence micrographs of MEF cells incubated with APDs confirms that APDs can be endocytosed by MEF cells and that the dots distribute throughout the cell cytoplasm (Fig. 5A and B). Because PDs are compatible with common excitation sources spanning the visible spectrum, they offer many options for multicolor and multiplex detection. In demonstration of this, we show in Fig. 5A and B that fluorescence signal can be monitored in either the green (FITC filter set) or the red (TRITC) spectral regions, providing contrast to the blue-fluorescing 4′,6-diamidino-2-phenylindole (DAPI) stain known to bind strongly to A-T rich regions in DNA.

Cytotoxicity screening versus the BT-474 cancer cell line was also carried out using a sulforhodamine B colorimetric assay for PD concentrations ranging from 0.05 to 1.5 mg mL^{-1} (Fig. 5C). There was full retention of cell viability at concentrations of 0.15 mg mL^{-1} for all three types of PDs. Further, the cytotoxicities of UPDs and CPDs were found to be negligible at PD concentrations as high as 0.5 mg mL^{-1}. Even at the highest PD concentration studied (1.5 mg mL^{-1}; it should be noted that prior studies of C-dot cytotoxicity have rarely included concentrations beyond 0.1–0.5 mg mL^{-1}), BT-474 cell cultures retained 90% of their viability. In fact, some of this apparent decrease in cell survival can be attributed to the osmotic shock associated with addition of relatively large volumes of the PD stocks (which were prepared in deionized water) to the 96-well plates used in the cytotoxicity screen. The resulting change in cell culture media osmolality can induce cell rupture which is not related to PD toxicity as such. Measurements at the lower PD concentrations were not subject to this artifact since miniscule volumes of PD solution were required for these concentrations. Regardless, the PDs appear to be highly biocompatible, even at high concentrations well in excess of those required for cellular imaging studies.

A final set of experiments investigated the utility of PDs in fluorescence-based metal ion sensing (Fig. 6 and S4†). In these experiments, PD fluorescence quenching behaviour was screened against 11 different metal ions: Zn^{2+}, Sr^{2+}, Ba^{2+}, Mn^{2+}, Ca^{2+}, Sn^{2+}, Ni^{2+}, Fe^{3+}, Cu^{2+}, Pd^{2+}, and Hg^{2+}. All three types of PD responded in a similar manner to each particular metal ion. The metal ions Zn^{2+}, Sr^{2+}, Ba^{2+}, Mn^{2+}, and Ca^{2+} showed no quenching of PD emission whilst Sn^{2+} and Ni^{2+} showed relatively weak quenching. The remaining metal ions (Fe^{3+}, Cu^{2+}, Pd^{2+}, and Hg^{2+}) all produced much stronger fluorescence quenching, with Pd^{2+} and Hg^{2+} displaying the strongest quenching capabilities of the metals tested, irrespective of the PD identity. Since the strongest quencher (Pd^{2+}) is an unlikely environmental contaminant in most waters, we focused our attention on investigating Hg^{2+} detection. Fig. 6A provides a representative Stern–Volmer plot of Hg^{2+} induced quenching of APD fluorescence, where F_0 and F represent the fluorescence intensities in the absence and presence of Hg^{2+}, respectively. Following the 3σ convention, the limit of detection (LOD) for a particular metal ion was determined as the [Hg^{2+}] concentration corresponding to a signal that differed from that of the metal-free result by thrice the standard deviation of the signal

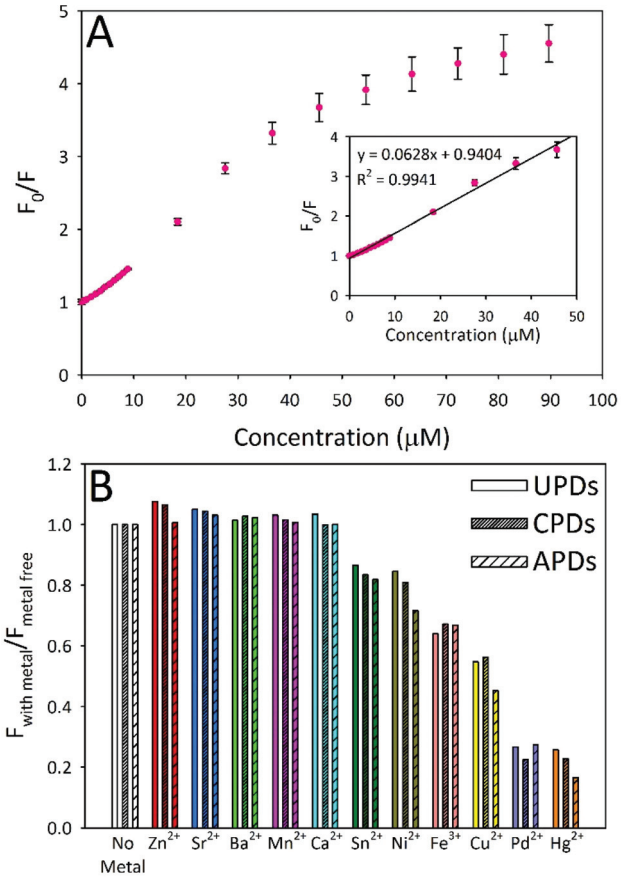

Fig. 6 (A) Representative plot of Hg^{2+} quenching of APD emission. (B) Metal screening test for all three PD types (0.05 mg mL^{-1}) against 11 different metal ions (Zn^{2+}, Sr^{2+}, Ba^{2+}, Mn^{2+}, Ca^{2+}, Sn^{2+}, Ni^{2+}, Fe^{3+}, Cu^{2+}, Pd^{2+}, and Hg^{2+}), each present at a concentration of 100 μM.

in the absence of metal. LOD values were estimated in the low micromolar range for both Hg^{2+} and Cu^{2+} ions. For UPDs, the calculated LODs were 2.7 μM and 3.4 μM for Hg^{2+} and Cu^{2+}, respectively. The corresponding Hg^{2+} (Cu^{2+}) LOD values for CPDs and APDs were 1.8 μM (1.7 μM) and 2.7 μM (2.9 μM), respectively.

In addition to showing quenchometric sensing capabilities for priority heavy metal ion pollutants, the fluorescence signal was almost completely (94–97%) recoverable through the addition of the strong metal-chelating agent ethylenediaminetetraacetic acid (EDTA) to Hg^{2+}-quenched samples (Fig. S5†).[33] An excess of EDTA (>4 : 1 EDTA : Hg^{2+} molar ratio) is required to achieve the greatest signal recovery, indicating that while a majority of the Hg^{2+} ions may be loosely interacting with the functional groups at the PD surface, some fraction are apparently bound with a high affinity.

Experimental

Roughly one liter of urine was collected for each of the three different dietary conditions investigated: unmodified diet,

vitamin C supplemented, and asparagus-rich diet. Since multiple excretions were required to acquire this volume, multiple fractions were pooled over the course of several days (collected between mid-morning and mid-afternoon) and homogenized to ensure a representative sample. In order to fortify the diet with vitamin C, four 500 mg vitamin C tablets (Nature Made Nutritional Products) were taken at 2 h intervals, with vitamin C-enriched urine collected 4 h and 6 h after consumption of the first tablet. To set the conditions for asparagus-urine, approximately one pound of lightly steamed locally-sourced fresh asparagus was consumed and urine collected within 6 h of its consumption. This exercise was repeated several times over the course of a couple days, much to the student's chagrin.

To initiate carbon dot synthesis, 450 g of a particular urine sample was dehydrated within a heated round-bottom flask immersed within an improvised sand bath consisting of an anodized aluminum round cake pan (Fat Daddio's) filled with copper-coated airgun BBs (0.177 caliber; Crosman Copperhead). Temperature control was achieved to within 2 °C using a digital stirring hotplate (Super-Nuova™; Thermo Scientific™) connected to a J-type thermocouple immersed in the BBs. Stirring was provided at 300 rpm using a PTFE-coated magnetic stir bar. The dehydrated residues were heated for an additional 12 h at 200 °C to yield a black char which readily resuspended in water. As the liquid evaporated, the urine gradually darkened from yellow to dark orange and, finally, a viscous brown solution. Throughout the carbonization process, the material evolved in appearance, eventually becoming a coal black. Following the carbonization step, the solid was reconstituted using 60 mL of water. The suspension was centrifuged at 5000 rpm for 30 min to remove large particles, filtered using a 0.45 μm nylon syringe filter (Fisherbrand, #09-719D), and then dialyzed for 12 h against 1.5 L of water (changing the dialysis water three times throughout) using 1 K MWCO cellulose dialysis tubing (Spectrum Labs Spectra/Por 7 Dialysis membrane, #132105). A portion of each dialyzed sample was freeze-dried in order to obtain a solid product for XRD analysis. Additional experimental details can be found in the ESI.†

Conclusions

To sum, we have shown that analytically useful and biocompatible fluorescent carbon dots can be facilely derived from the thermal upcycling of human urine. The synthesized pee dots were found to be effective nanoscale labels, illustrated in the multiplexed fluorescence imaging of mice embryonic fibroblast cells, whilst showing no apparent cytotoxicity at concentrations approaching 1.5 mg mL^{-1}. These dots also proved to be excellent nanosensors for the fluorescence quenching-based detection of priority heavy metal ion pollutants of environmental interest like mercuric ion (Hg^{2+}). The fluorescence signal was fully recoverable using EDTA as a chelator, suggesting the potential for immobilization of the dots within reusable paper test strips for water quality monitoring, for example.

The current work represents one of the few instances where fluorescent quantum yields have been measured for a multiplicity of wavelengths for C-dots. Our findings reveal a marked decrease in quantum yield with excitation wavelength, suggesting a need to shift away from reporting quantum yields at a single excitation wavelength (*e.g.*, 350 nm) or, at the very least, to employing visible excitation wavelengths better matched to target applications such as bioimaging, sensing, and photovoltaics for which the C-dots are being proposed for immediate exploitation. Moreover, this observation points to the need to specify the precise optical conditions employed when making meaningful comparisons between quantum yields and other optical properties commonly reported in the literature, a guideline not always followed. Pragmatically, another consequence of these findings is that C-dots that yield the highest emission under ultraviolet or blue emission may not necessarily be those best suited for practical bioimaging, particularly given the excitation of cellular autofluorescence in these spectral regions.

Intriguingly, we have also demonstrated that the fluorescent, size, and sensory characteristics of the carbon dots can be modulated by simple dietary modifications of the urine donor. For instance, intentional consumption of sulfur-containing foodstuffs (*i.e.*, asparagus) was shown to lead to measurable red shifts in the fluorescence emission from the dots. Although highly speculative, this result suggests the enticing notion that an extension of this approach might possibly be used to assess the diet and general health of urine donors in resource-limited settings, as such will be reflected in the optical features of the subsequent dots produced to some extent. In any case, we provide compelling evidence that urine can be upcycled into a useful carbonaceous product in a process that could potentially combine, simplify, or remove steps in wastewater treatment. Within a larger context, the work adds momentum to research aimed at upcycling low or negatively-valued waste into useful and compelling nanocarbons.

Conflict of interest

The authors declare no competing financial interest.

Acknowledgements

This work was supported by the Interdisciplinary Intercampus (IDIC) Research Program at the University of Missouri. We thank Dr Tommi White and the MU Electron Microscopy Core Facility for the provision of imaging resources. We are grateful to Prof. Jian "Javen" Lin (Department of Mechanical & Aerospace Engineering) for stimulating discussions on the future of this exciting area.

Notes and references

1 S. N. Baker and G. A. Baker, *Angew. Chem., Int. Ed.*, 2010, **49**, 6726–6744; J. B. Essner, C. H. Laber and G. A. Baker, *J. Mater. Chem.*, 2015, **3**, 16354–16360.
2 C. Ding, A. Zhu and Y. Tian, *Acc. Chem. Res.*, 2013, **47**, 20–30.
3 H. Li, Z. Kang, Y. Liu and S.-T. Lee, *J. Mater. Chem.*, 2012, **22**, 24230–24253.
4 J. Shen, Y. Zhu, X. Yang and C. Li, *Chem. Commun.*, 2012, **48**, 3686–3699.
5 J. Wang, X. Xin and Z. Lin, *Nanoscale*, 2011, **3**, 3040–3048.
6 Z. Zhang, J. Zhang, N. Chen and L. Qu, *Energy Environ. Sci.*, 2012, **5**, 8869–8890.
7 X. Xu, R. Ray, Y. Gu, H. J. Ploehn, L. Gearheart, K. Raker and W. A. Scrivens, *J. Am. Chem. Soc.*, 2004, **126**, 12736–12737.
8 S.-L. Hu, K.-Y. Niu, J. Sun, J. Yang, N.-Q. Zhao and X.-W. Du, *J. Mater. Chem.*, 2009, **19**, 484–488.
9 Y.-P. Sun, B. Zhou, Y. Lin, W. Wang, K. A. S. Fernando, P. Pathak, M. J. Meziani, B. A. Harruff, X. Wang, H. Wang, P. G. Luo, H. Yang, M. E. Kose, B. Chen, L. M. Veca and S.-Y. Xie, *J. Am. Chem. Soc.*, 2006, **128**, 7756–7757.
10 H. Li, X. He, Z. Kang, H. Huang, Y. Liu, J. Liu, S. Lian, C. H. A. Tsang, X. Yang and S.-T. Lee, *Angew. Chem., Int. Ed.*, 2010, **49**, 4430–4434.
11 H. Ming, Z. Ma, Y. Liu, K. Pan, H. Yu, F. Wang and Z. Kang, *Dalton Trans.*, 2012, **41**, 9526–9531.
12 Q.-L. Zhao, Z.-L. Zhang, B.-H. Huang, J. Peng, M. Zhang and D.-W. Pang, *Chem. Commun.*, 2008, 5116–5118.
13 L. Zheng, Y. Chi, Y. Dong, J. Lin and B. Wang, *J. Am. Chem. Soc.*, 2009, **131**, 4564–4565.
14 J. Zhou, C. Booker, R. Li, X. Zhou, T.-K. Sham, X. Sun and Z. Ding, *J. Am. Chem. Soc.*, 2007, **129**, 744–745.
15 A. B. Bourlinos, A. Stassinopoulos, D. Anglos, R. Zboril, V. Georgakilas and E. P. Giannelis, *Chem. Mater.*, 2008, **20**, 4539–4541.
16 Y. Yang, D. Wu, S. Han, P. Hu and R. Liu, *Chem. Commun.*, 2013, **49**, 4920–4922.
17 S. Qu, X. Wang, Q. Lu, X. Liu and L. Wang, *Angew. Chem., Int. Ed.*, 2012, **51**, 12215–12218.
18 Q.-Q. Shi, Y.-H. Li, Y. Xu, Y. Wang, X.-B. Yin, X.-W. He and Y.-K. Zhang, *RSC Adv.*, 2014, **4**, 1563–1566.
19 P.-C. Hsu, Z.-Y. Shih, C.-H. Lee and H.-T. Chang, *Green Chem.*, 2012, **14**, 917–920.
20 W. Lu, X. Qin, S. Liu, G. Chang, Y. Zhang, Y. Luo, A. M. Asiri, A. O. Al-Youbi and X. Sun, *Anal. Chem.*, 2012, **84**, 5351–5357.
21 J. Zhou, Z. Sheng, H. Han, M. Zou and C. Li, *Mater. Lett.*, 2012, **66**, 222–224.
22 M. A. Shannon, P. W. Bohn, M. Elimelech, J. G. Georgiadis, B. J. Marinas and A. M. Mayes, *Nature*, 2008, **452**, 301–310.
23 X. Cao, L. Ma, B. Gao and W. Harris, *Environ. Sci. Technol.*, 2009, **43**, 3285–3291.
24 Q. Qian, M. Machida and H. Tatsumoto, *Waste Manage.*, 2008, **28**, 1064–1071.
25 J. Wei, X. Zhang, Y. Sheng, J. Shen, P. Huang, S. Guo, J. Pan, B. Liu and B. Feng, *New J. Chem.*, 2014, **38**, 906–909.
26 J. Werther and T. Ogada, *Prog. Energ. Combust.*, 1999, **25**, 55–116.
27 S. Larson, Is "Pee-cycling" the Next Wave in Sustainable Living?, http://news.nationalgeographic.com/news/2014/02/140202-peecycling-urine-human-waste-compost-fertilizer/, (accessed May 10, 2015).
28 G. Lawton, *New Scientist*, 2006, **192**, 45–47.
29 V. G. Pol, *Environ. Sci. Technol.*, 2010, **44**, 4753–4759.
30 G. Ruan, Z. Sun, Z. Peng and J. M. Tour, *ACS Nano*, 2011, **5**, 7601–7607.
31 F. Müller, S. Grandthyll, S. Gsell, M. Weinl, M. Schreck and K. Jacobs, *Langmuir*, 2014, **30**, 6114–6119.
32 L. Minzae, K. Gil-Pyo, S. Hyeon Don, P. Soomin and Y. Jongheop, *Nanotechnology*, 2014, **25**, 345601.
33 S. Liu, J. Tian, L. Wang, Y. Zhang, X. Qin, Y. Luo, A. M. Asiri, A. O. Al-Youbi and X. Sun, *Adv. Mater.*, 2012, **24**, 2037–2041.
34 S.-S. Liu, C.-F. Wang, C.-X. Li, J. Wang, L.-H. Mao and S. Chen, *J. Mater. Chem. C*, 2014, **2**, 6477–6483.
35 N. K. Chaudhari, M. Y. Song and J.-S. Yu, *Sci. Rep.*, 2014, **4**, 5221.
36 S. C. Mitchell, *Drug Metab. Dispos.*, 2001, **29**, 539–543.
37 M. L. Pelchat, C. Bykowski, F. F. Duke and D. R. Reed, *Chem. Senses*, 2011, **36**, 9–17.
38 R. H. Waring, S. C. Mitchell and G. R. Fenwick, *Xenobiotica*, 1987, **17**, 1363–1371.
39 R. White, *Science*, 1975, **189**, 810–811.
40 Y. Mao, Y. Bao, L. Yan, G. Li, F. Li, D. Han, X. Zhang and L. Niu, *RSC Adv.*, 2013, **3**, 5475–5482.
41 M. Xie, Y. Su, X. Lu, Y. Zhang, Z. Yang and Y. Zhang, *Mater. Lett.*, 2013, **93**, 161–164.
42 W. F. Zhang, H. Zhu, S. F. Yu and H. Y. Yang, *Adv. Mater.*, 2012, **24**, 2263–2267.
43 Y. Dong, J. Shao, C. Chen, H. Li, R. Wang, Y. Chi, X. Lin and G. Chen, *Carbon*, 2012, **50**, 4738–4743.
44 A. Philippidis, A. Spyros, D. Anglos, A. Bourlinos, R. Zbořil and E. Giannelis, *J. Nanopart. Res.*, 2013, **15**, 1–9.
45 R. Ye, C. Xiang, J. Lin, Z. Peng, K. Huang, Z. Yan, N. P. Cook, E. L. G. Samuel, C.-C. Hwang, G. Ruan, G. Ceriotti, A.-R. O. Raji, A. A. Martí and J. M. Tour, *Nat. Commun.*, 2013, **4**, 2943.

